Olefin Methylation over Iron Zeolites and the Methanol to Hydrocarbons Reaction

Mark LaFollette, [a, b] and Raul F. Lobo*[a, b]

[a] Catalysis Center for Energy Innovation, Department of Chemical and Biomolecular Engineering, University of Delaware, Newark, Delaware 19716, United States

[b] Department of Chemical and Biomolecular Engineering, University of Delaware, Newark, Delaware 19716, United States

*Corresponding Author: lobo@udel.edu

Abstract

The effect of olefin addition to a stream of dimethyl ether on the methanol homologation reaction is investigated using iron-substituted zeolites Fe-beta and Fe-ZSM-5. The reaction was investigated using plug-flow microreactors in the temperature range of 240-400 °C, at a total pressure of 0.239 MPa and a WHSV of 6.12 (g DME/g_{cat}-hr). For Fe-beta (Si/Fe= 9.2) catalysts, isobutene co-feeding almost doubles dimethyl ether (DME) consumption rate and shifts selectivity towards larger olefins with carbon numbers from 5-7. Addition of isobutene above 6.3%, however, resulted in a reduction of DME consumption rates, an effect assigned to the replacement of surface methoxy groups for adsorbed olefins in the zeolite pores. Below a temperature of 340 °C hydride-transfer rates are negligible; reaction rates are stable for over 5.5 hours and the products consist almost exclusively of olefins and a small amount of methane. Above 360 °C the onset of catalytic hydride transfer processes is observed leading to fast catalyst deactivation rates and an increase in the concentration of aromatic species. Iron ZSM-5 (Si/Fe= 21.4) catalysts under similar reaction conditions consumes methanol faster than Fe-beta at approximately three times the TOF (on a per iron basis). The Fe-ZSM-5 catalyst was selective to a distribution of products (C5 to C8) as compared to Fe-beta which was selective to primarily C5 and C7. Co-feeding larger olefins (2-methyl-2-butene, 2,3-dimethyl-2-butene, 2,3,3-trimethyl-1-butene, and 2,4,4-trimethyl-2-pentene) at a 3.9% olefin concentration over Fe-beta changed selectivity towards cracking products (C4 compounds such as isobutene). As the size of the olefin increases, a reduction of DME consumption rate is also observed. These results show that co-feeding olefins with DME over Fe-zeolites is a promising route to increase methylation rates at relatively low temperatures producing larger branched olefins and that the product distribution is highly dependent on the zeolite pore size and structure of the olefin.

Keywords: Iron Zeolite, Methylation Reaction, Methanol Homologation, Methanol to Hydrocarbon, Methanol to Olefin

1. Introduction

Methanol and dimethyl ether (DME) can be converted into hydrocarbons by acidic zeolites via the methanol to hydrocarbon (MTH) process discovered by researchers at Mobil in the 1970s [1,2]. Methanol to hydrocarbon processes can be classified into two categories: methanol to gasoline (MTG) and methanol to olefins (MTO), depending on catalyst and operating conditions [3]. The primary products are olefins, paraffins, and aromatics for MTG, and light olefins, such as ethylene and propylene, for MTO. The product distribution in MTH is dependent on the zeolite structure and acidity [4].

The MTH reaction occurs through the so-called hydrocarbon pool mechanism, which is formed of two parallel reaction cycles denoted as the olefin cycle and the aromatic cycle [5–12]. In the olefin cycle, an olefin will undergo sequential methylations until it is large enough to crack into smaller olefins that re-enter the cycle. Alternatively, olefins can undergo hydride transfer reactions to form an alkane and a diene (or triene), which undergo cyclization and aromatization allowing these species to enter the aromatic cycle. In the aromatic cycle, the arene is either methylated or methyl groups are added to existing arene side chains until olefins (ethylene, propylene) are released. The coupling of methylated arenes into larger arenes is a likely mechanism of deactivation of the zeolite catalyst [13,14].

Pore structure and dimensions have a large effect on the product composition, and zeolite beta, a 3-dimensional large-pore zeolite, shows a distribution quite different from the one observed in ZSM-5. The beta zeolite is selective primarily to isobutane and triptane, while ZSM-

5 is selective to propane, ethane, and aromatics [15–18]. The high selectivity to C7 alkanes and alkenes in zeolite beta is directly related to the larger pore size which allows for rapid diffusion of these larger compounds out of the zeolite pores.

Isomorphous substitution of several metals into a zeolite framework during synthesis leads to changes in acid strength [19–22]. Jones et al.[23] measured the rate of methanol dehydration over isomorphous substituted MFI containing Al, Fe, Ga, and B and found that the rate constants increased with increasing acid strength as calculated by deprotonation energy. Using this metric, substituted iron zeolite had a weaker acidity than the aluminum zeolite (but of the same order of magnitude) and a rate constant two orders of magnitude larger than the boron catalyst.

Iron zeolites (H-[Fe]ZSM-5) are, [24,25] compared to aluminum zeolites, significantly more selective to alkenes than alkanes and aromatics in MTH chemistry. They increase the propylene selectivity while decreasing the ethylene selectivity favoring the olefin cycle over the aromatic cycle [26]. These changes in selectivity are caused by the lower acidity of iron zeolites hindering hydride transfer reactions and preventing alkane formation and the subsequent formation of aromatic species. Nonetheless, iron zeolites also have lower reaction rates than aluminum zeolites of similar silicon to framework metal ratios due to their weaker acidity and its impact on the reaction's activation energy.

Co-feeding olefins or aromatic species in the MTH reaction has been investigated to determine kinetic parameters and to define reaction mechanisms [15,27–32]. Co-feeding olefins changes selectivity and increases reaction rate in aluminosilicate zeolite catalysts [33–36]. Over H-ZSM-5, Wu et al. [37] found that co-feeding alcohols, which convert dehydrate to form normal olefins, increased the MeOH conversion, particularly with 1-butanol and 1-pentanol.

Huang et al. [38] found that oven ZSM-5 with an olefin co-fed the dominant reaction pathway is the olefin methylation and cracking reactions of the olefin cycle. Sun et al. [36] found that although the reaction rates increased upon co-feeding olefins, the aromatic cycle was still partially active, and the selectivity to ethylene remained the same. Erichsen et al. [39] compared methylation rates and product selectivity of co-fed benzene over two catalysts, a zeolite and a SAPO with the AFI framework type. The olefins produced by the zeolite were mainly ethylene and some propylene, whereas the SAPO produced larger C4 and C5 olefins and had higher olefin selectivity. This difference in selectivity is believed to be due to SAPOs weaker acid strength than aluminum zeolites, although, they can contain acid sites that are of similar strength [40,41].

We report an investigation of the effect of co-feeding olefins in the MTH reaction over iron-containing zeolite catalysts. Addition of isobutene to the feed increases the rate of the MTH reaction over an iron beta zeolite catalyst and shifts the selectivity to a pool of C4-C7 olefins. Co-feeding of C5-C8 olefins—selected from the methylation pathway of the olefin cycle over aluminum zeolites—were used to understand the reaction mechanism and the impact of the olefin on selectivity. Iron zeolites can be used as a methylation catalyst to selectively methylate olefins towards larger species generating an olefin pool with a composition that can be changed by the catalyst framework and by the olefin that is co-fed.

2. Experimental

2.1 Zeolite Synthesis

H-[Fe]beta was prepared using the method reported by Raj et al. [42] with a synthesis gel composition of 0.59 Na_2O:0.30 K_2O: 0.58 Fe_2O_3:30 SiO_2:15 TEAOH:355 H_2O. First, a solution was prepared by dissolving (6.70 g, Cab-o-sil) fumed silica in a solution of (0.17 g, Fisher) NaOH, (0.13 g, Fisher) KOH, and (23.60 g, 35% Alfa Aesar) tetraethylammonium hydroxide solution. A second solution was made with (1.05 g $Fe_2(SO_4)_3 \cdot 5H_2O$, Arcos Organics) Iron (III) sulfate dissolved in (8.24 g) deionized (DI) water. The second solution was then added to the first solution and mixed. Seed crystals (0.11 g) were then added to the solution and mixed. The seed crystals were prepared through successive dilution of the previous synthesis until no aluminum impurities were detected. The synthesis gel was then heated for 15 days at 413K statically in a 45 mL Teflon-lined Parr 4744 autoclave.

H-[Fe]ZSM-5 was prepared using the method reported by Yun et al. [43] with a synthesis gel composition of 30 Na_2O:0.19 Fe_2O_3:30 SiO_2:5 TPABr:1733 H_2O:22 H_2SO_4. First, a solution was prepared by adding (0.23 g) Iron (III) Sulfate, (5.5 g, Fisher) concentrated sulfuric acid, and (25 g) DI water and mixing. A second solution was prepared by dissolving (21.32 g, $Na_2SiO_3 \cdot 9H_2O$, Sigma Aldrich) sodium metasilicate in (40.85 g) DI water. The second solution was then added slowly to the first solution while mixing. Next, (3.33 g, 98% Sigma Aldrich) tetrapropylammonium bromide was added to the mixed solutions while stirring. The solution was then transferred to Teflon-lined parr autoclaves. The autoclaves were rotated for three days at 170°C.

Upon the completion of synthesis, the zeolites were recovered through centrifugation and then were washed with deionized water until the filtrate had a neutral pH. After drying overnight at 80°C, the zeolites were in the "as-made" form. The zeolites were then calcined in air to remove the structure-directing agents; gradual heating rates were used to help the Fe remain in the framework. Fe-beta was calcined by using a 2.2 °C/min ramp rate to 150 °C, hold for 2 hours, a ramp of 1.8°C/min to 480 °C, and hold for 5 hours. Fe-ZSM-5 was calcined using a 2°C/min ramp rate to 480 °C and held for 4 hours.

The calcined zeolites were then ion-exchanged overnight at room temperature with an ammonium nitrate solution. Fe-beta used a 0.05 M ammonium nitrate solution with the mass of ammonium nitrate equal to five times the mass of iron sulfate in the synthesis gel. Fe-ZSM-5 used 500 mL of 0.1 M ammonium nitrate solution per 1 gram of zeolite. The zeolites were then centrifuged to remove the ammonium nitrate and washed with deionized water three times before drying overnight at 80 °C to yield the ammonium form.

2.2 Characterization

Powder X-ray diffraction (XRD) patterns were collected on a Bruker D8 X-ray diffractometer with a Cu Kα source (λ=1.542 Å). Diffraction patterns were measured using a step size 0.05° 2θ with the time per step of 0.5 sec between the angles of 5° to 50° 2θ. The elemental composition of the zeolites was determined by ICP-OES done by Galbraith laboratories (Knoxville, TN, USA). A Jasco V-550 UV/Vis Spectrometer was used to measure the diffuse reflectance UV/Vis spectra of the as-made and calcined iron zeolite samples. UV/Vis spectra were measured with a scan rate of 400 nm/min between the wavelengths of 220 nm and 850 nm. Nitrogen desorption isotherms were measured on a Micromeritics 3Flex Physisorption instrument to determine the micropore volume via the t-plot method. The samples were

pretreated with a 1°C/min heating rate to 150 °C at a pressure of 0.5 torr overnight. The SEM images were obtained on a JEOL JSM7400F microscope with an acceleration voltage of 3 keV and 10 μA.

2.3 Catalytic Properties of Fe-zeolites

The methylation reactions were carried out in a packed bed reactor comprised of a 0.25 inch 316 stainless steel tube with a 0.035 inch wall thickness. The zeolite powder, in its ammonium form, was pressed, crushed, and sieved (40-60 mesh) to particle sizes between 250-425 μm. 200 mg of catalyst was converted in situ to the hydrogen form. For Fe-beta a heating rate of 2 °C /min was used from room temperature to 400 °C and held for 8 hours with flowing air (100 SCCM) to get the acid (H) form of the sample. For Fe-ZSM-5 a heating rate of 2°C/min was used up to 200 °C and held for 2 hours; then a heating rate of 2°C/min was used to get to 480 °C and was held for 3 hours under flowing nitrogen (100 SCCM) to obtain the H+-form.

An online Agilent 7890B Gas Chromatograph (GC) with a flame ionization detector (FID) was used to analyze the reactor effluent composition. The GC was equipped with an Agilent HP-PlotQ column (30m x 320 μm ID, 0.20 mm film thickness). Methanol was counted as unreacted feed for calculating conversion, DME consumption rate, and the carbon selectivity. The co-fed olefin was excluded from the carbon selectivity due to not being able to differentiate between generated and co-fed olefin (further justification provided in the supplemental information). Carbon balances were calculated without accounting for ethane which served as an internal standard. The feed gas consisted of a carrier gas mixture of 99% helium and 1% ethane (Praxair), DME (Sigma-Aldrich 99%), and isobutene (Sigma-Aldrich). Olefins (Figure 1) such as 2-methyl-2-butene (Sigma Aldrich), 2,4-dimethyl-2-butene (Sigma Aldrich), 2,3,3 trimethyl-1-

butene (Sigma Aldrich), and 2,4,4-trimethyl-2-pentene (Sigma Aldrich) were co-fed into the reactor using a New Era Pump Systems NE-1000 syringe pump.

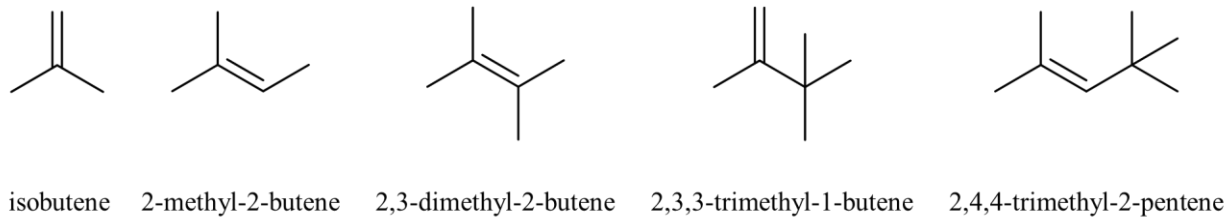

Figure 1 Co-fed olefins structure

Catalysis experiments were conducted at a pressure of 0.239 MPa maintained by a Swagelok back pressure regulator (KBP1E0A4D5A60000) and with a weight hourly space velocity (WHSV) of 6.12 $g_{DME}g_{cat}^{-1}h^{-1}$. The MTH reaction and isobutene co-fed reaction were both preformed at 300 °C over H-[Fe]beta. The concentration percentage reported for olefin co-feeds is the percent of reactants that are olefin on a total olefin and DME molecular molar basis. The isobutene co-fed amount varied from 3.9 to 24.4% over H-[Fe]Beta at 300°C. The reaction temperature was changed in 20 °C increments from 240 °C to 400 °C for isobutene methylation at a 6.3% isobutene co-fed amount over H-[Fe]beta. The isobutene dimerization rate was investigated in the same carrier gas as above over H-[Fe]beta at 300 °C with the same total flow, isobutene flow rate, and amount of catalyst as the 24.4% isobutene co-fed with DME. The isobutene co-fed reaction using an isobutene co-fed of 6.3% and the MTH reaction at similar conditions were measured over H-[Fe]ZSM-5 at 300 °C, 0.239 MPa, and a WHSV of 6.12 $g_{DME}g_{cat}^{-1}h^{-11}$.

3. Results and Discussion

3.1 Material Characterization

The samples of Fe-beta and Fe-MFI were prepared based on previous reports and the details of the synthesis protocols are found in the Experimental section 2.1 [42,43]. The XRD pattern for the as-made Fe-beta (Figure S1A) is fully consistent with a faulted intergrowth of polytypes BEA and BEB and contains both broad and sharp diffraction peaks as is observed for Al-beta. The XRD pattern for the as-made Fe-ZSM-5 (Figure S1B) is also fully consistent with the pattern of ZSM-5[44]. No crystalline impurities were identified in the XRD patterns. The nitrogen adsorption isotherms (Figure S2) were c type IV isotherms [45]. The micropore volumes, calculated using the t-plot method were 0.22 cm^3g^{-1} for NH_4-[Fe]beta and 0.12 cm^3g^{-1} for NH_4-[Fe]MFI. These are both comparable to the microporous aluminosilicate analogues for each framework-type [43,46]. The Si/Fe ratio was determined by ICP-OES spectroscopy and was 9.2 for as-made Fe-beta and Si/Fe ratio of 21.4 for Fe-ZSM-5. The Si/Al ratio for Fe-ZSM-5 was 1226 and the aluminum concentration for Fe-beta was below the ICP detection limit (Si/Al >

11,324).

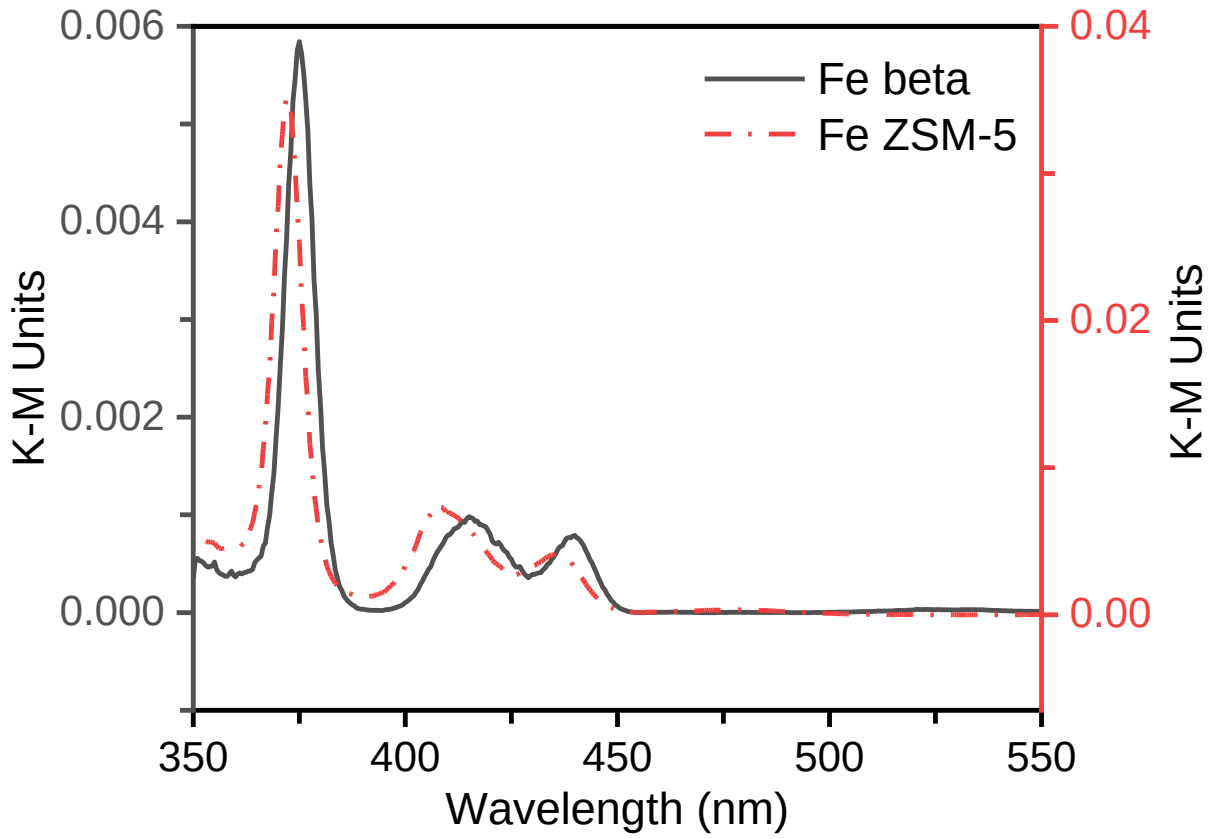

Figure 2 UV/vis spectra of as made Fe Beta (Solid, left y-axis) and as made Fe ZSM-5 (Dashed, right y-axis) both showing peaks characteristic of d-d electron transitions for iron (III) in a tetrahedral environment

The UV/Vis spectra for the as-made zeolite samples confirm the isomorphous substitution of Fe for Si in both zeolite frameworks (Figure 2). The UV/Vis spectrum of isolated iron Fe^{3+} in a tetrahedral configuration, as in the zeolite framework, has 4 electronic transitions

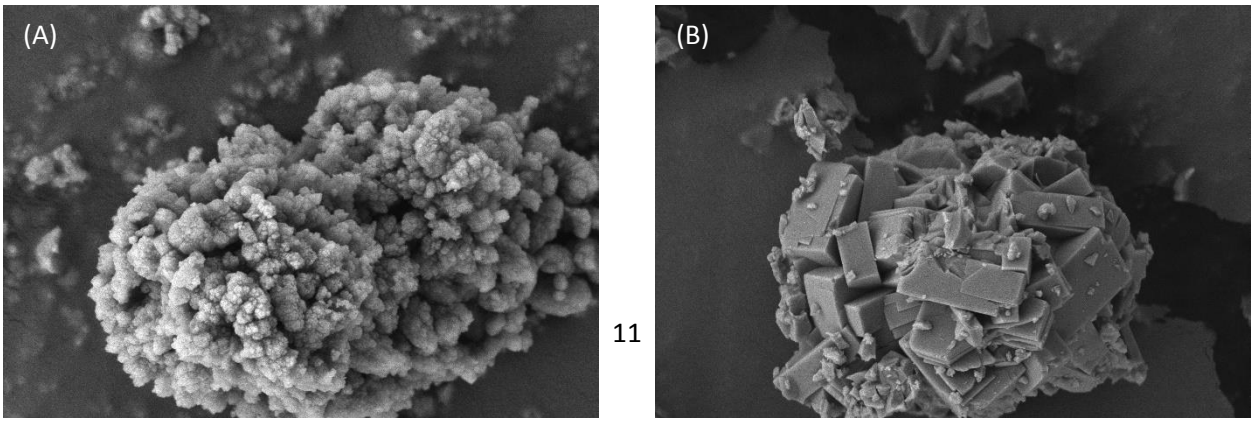

Figure 1 SEM Images of Iron Zeolites (A)NH_4[Fe]beta (B)NH_4[Fe]ZSM-5

around 375 nm, 415 nm, 440 nm, and 480 nm, although, the peak at 480 nm is not always observed [47–49]. These peaks correspond to the d-d electronic transitions when Fe^{3+} is in a tetrahedral coordination environment and thus Figure 2 confirms that the initial samples have iron isomorphously substituted in the framework. After the zeolites were calcined to remove the structure-directing agent (SDA), a slight color change from white to a light off-white color was observed. The color change was more apparent for Fe beta as compared to Fe ZSM-5. This change is reflected in the UV/Vis spectra of the calcined samples that show an intensity reduction of the tetrahedral absorption peaks (Figure S3). This spectral evolution has been often reported in the literature and has been assigned to a small amount of iron leaving the framework and forming extra-framework iron oxide species [48,50].

The SEM image of the NH_4-[Fe]beta (Figure 3A) shows that this powder sample has a polycrystalline morphology of aggregated smaller particles under a quarter of a micron. The SEM image of NH_4-[Fe]ZSM-5 (Figure 3B) shows that this sample also consists of particles that are aggregates of smaller crystals, a different morphology from the typical coffin like morphology seen in many ZSM-5 samples. NH_4-[Fe]ZSM-5 has larger particles than NH_4-[Fe]beta. The intracrystalline space between the crystal aggregates is probably responsible for the small amount of microporosity observed in the isotherms for both iron zeolites (Figure S2).

The characterization data show that the samples have only the desired zeolite frameworks with most of the iron in the framework. The amount of aluminum impurities present in the samples is very small and thus, the catalytic properties reported below are primarily due to the Brønsted acid sites present in iron zeolites.

3.2 Effect of Isobutene Co-fed on Rates and Selectivity

The direct MTH reaction rate is very low over iron zeolites and a strategy to enhance the rate is by co-feeding olefins that, in turn, enhance the olefin cycle rates. At low temperatures (≤ 260 °C) where the rate of MTH is very low, reaction rates increase by a factor of ~3 upon the addition of 6.4% isobutene to the feed gas, and once the isobutene is stopped the reaction rate decreased back rapidly to its original value (Figure S4). This rate increase occurs not only because the olefins fed to the reactor are methylated, but also because cracking of the larger olefins increase olefin concentration leading to an autocatalytic effect that can also enhance reaction rates. If the catalyst cannot generate olefins at a high enough rate, the olefin cycle cannot operate, and this carbon pool is lost by diffusion. Once olefins are co-fed the reaction rate increases, and the olefin cycle can get underway at a much faster rate. The reduction in DME consumption rate to the initial value suggests that it is not only the slower rate of formation of olefins from DME causing the low reaction rates of iron zeolites. *Note also that the products consists of almost exclusively olefins; no aromatics were detected and the only alkane was methane.*

The normal MTH reaction (no olefins) and MTH + isobutene reaction were conducted over an H-[Fe]beta catalyst at 300 °C (Figure 4A). The addition of isobutene leads to almost doubling the DME consumption rate, consistent with previous reports over Al-zeolites that show that the co-feeding of olefins increase methanol consumption rates at low conversions [36,37]. In this case, increasing the DME consumption rate by co-feeding isobutene helps to overcome the lower reactivity typically observed in the less acidic Fe-zeolites with respect to the rates observed over Al-zeolites. Figure 4B compares the carbon selectivity of both isobutene methylation and the MTH reaction over H-[Fe]beta where it can be observed that isobutene

makes up nearly 90% of all the C4 products and almost 50% of the total carbon in the MTH reaction.

In contrast, for the reaction with an isobutene co-fed, the products are larger compounds (C5 and C7 primarily, but also C6 and C8s), a result of the sequential methylation of the isobutene. The increase in C3 products is the result of the cracking of larger olefins formed from successive methylations of isobutene. The high selectivity to C5s is consistent with C5s being the primary product of the methylation reaction of isobutene. No aromatic products were detected at these conditions. We observed a 95% selectivity to propylene over propane in the C3 fraction during the isobutene co-fed, and thus we conclude that hydride transfer reactions occur at a slow rate over H-[Fe]beta and that olefins are the main product.

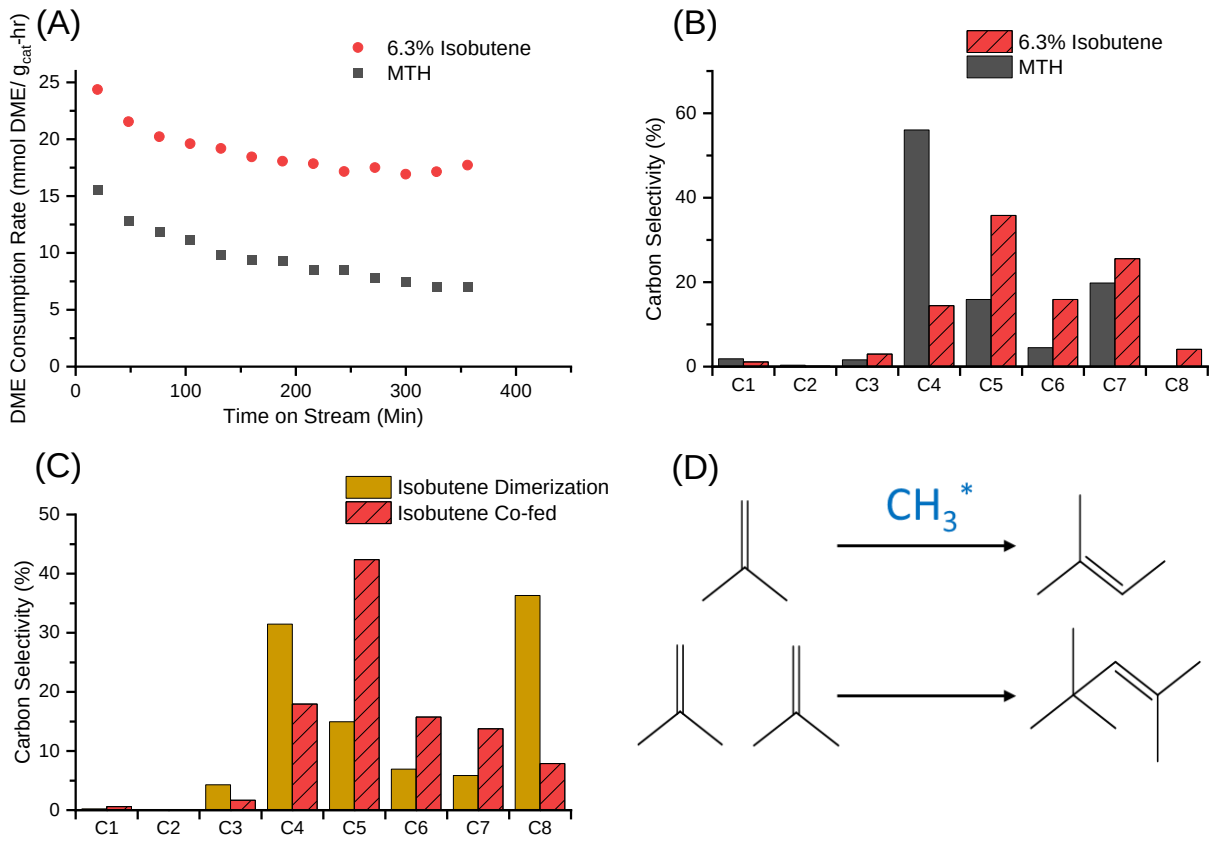

Figure 4 (A) DME consumption rate over H-[Fe]beta for MTH and DME co-fed with isobutene

at 300 °C, 0.239 MPa, and WHSV 6.12 $g_{DME}g_{Catalyst}^{-1}hour^{-1}$ 6.3% isobutene co-fed. (B) Carbon selectivity for MTH and DME co-fed with isobutene over H-[Fe]*b*eta after 216 minutes time on stream. (C) Carbon selectivity for isobutene dimerization and isobutene co-fed (24.4%) with DME over H-[Fe]beta after 216 minutes time on stream. Total flow rate and isobutene flow rate are the same for both the co-fed and dimerization reactions. Isobutene, the co-fed olefin, is not accounted for in carbon selectivity due to not being able to differentiate between generated and co-fed isobutene. (D) Isobutene methylation reaction and dimerization reaction. CH_3* is a surface methoxy group. Carbon balance at 216 minutes time on stream MTH 94%, 6.3% isobutene 95%, and isobutene dimerization 93%.

Olefin dimerization (i.e., alkylation) occurs over zeolites at temperatures as mild as 40 °C for isobutene although these particular experiments were done in the liquid phase and higher pressures [51,52]. The selectivity for an isobutene co-fed with DME is different than the pure isobutene oligomerization reaction over H-[Fe]beta (Figure 4C) at the same total flow rate and isobutene flow rate. Under our reaction conditions, dimerization to C8 olefins and formation of C4 isomers either from cracking or direct isomerization of the oligomerization products of isobutene (Figure 4D). DME + isobutene produces a pool of C5-C7 olefins, that is, the methylation rate of isobutene and larger olefins is significantly faster than the oligomerization rate. The selectivity to C8 olefins—which can form through either four successive methylations of isobutene or through an isobutene oligomerization reaction—has a carbon selectivity that is about five times smaller when DME is present, evidencing that multiple isobutene methylation reactions are occurring at faster rates than oligomerization. The preference of methylation reactions over oligomerization reactions of olefins over iron zeolites is similar to what has been observed for aluminum zeolites [37].

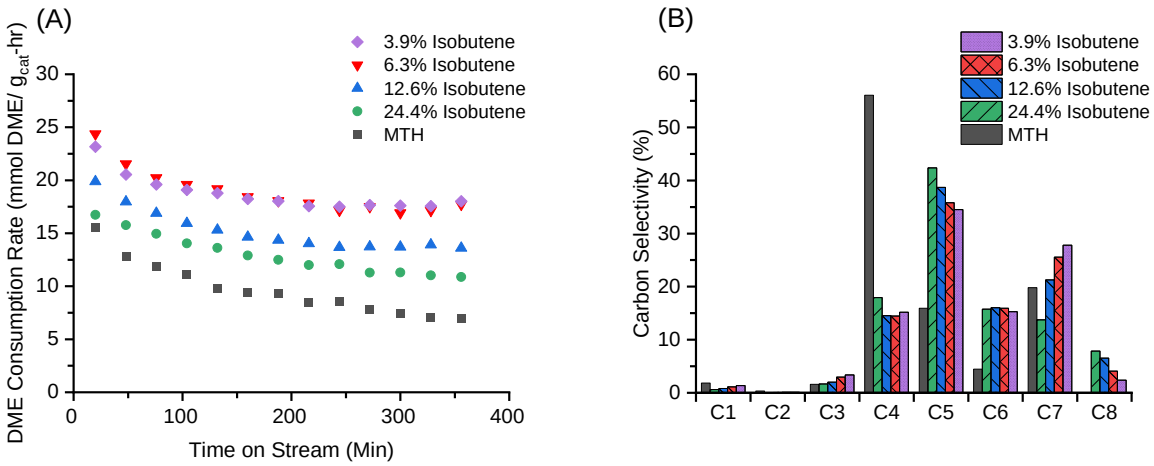

Figure 5 (A) DME consumption rate over H-[Fe]beta for the isobutene co-fed reaction at 300 °C, 0.239 MPa, and WHSV 6.12 $g_{DME}g_{Catalyst}^{-1}hour^{-1}$ with different isobutene feed amounts. (B) Carbon selectivity of isobutene co-fed over H-[Fe]beta with different isobutene feed amounts after 216 minutes time on stream. Carbon balance at 216 minutes time on stream 3.9% co-fed isobutene 100%, 6.3% co-fed isobutene 95%, 12.6% co-fed isobutene 94%, and 24.4% co-fed isobutene 94%.

Increasing the amount of isobutene co-fed reduces DME consumption rate (Figure 5A) although in all cases, DME consumption rate with isobutene co-fed is higher than rates under MTH conditions. This inverse relationship is different from the reaction of other olefins over aluminum zeolite catalysts. For example, Sun et al. [36] found that increasing pentene concentration from 2 to 8% of the feed (not counting inert carrier gas) led to an increase in methanol conversion over H-[Al]ZSM-5. The isobutene concertation of the feed (not counting inert carrier gas) changed from 3.9% to 24%. The change in isobutene from 3.9% to 6.3% had no effect on rate while increasing the feed to 12.6% and 24.4% decreased the reaction rate. This could be explained through a Langmuir-Hinshelwood-Hougen-Watson (LHHW) type model (see Equation) which has been shown to describe the olefin cycle of MTH [31]. As the amount of olefin co-fed increases, the rate decrease because the olefin saturates the zeolite acid sites.

$$rate \propto \frac{1}{1 + K_{DME} P_{DME} + K_{olefin} P_{olefin}}$$

The selectivity of the reaction (Figure 5B) shows that the isobutene co-fed is most selective to C5 with the selectivity to C5 increasing as the amount of co-fed isobutene increases. The higher selectivity to C5 and the decreasing reaction rate as the amount of isobutene increases can also be explained through LHHW kinetics. In the presence of DME, zeolites Bronsted acid sites react to form methoxy groups to an extent that depends on the local DME/water vapor pressure. When olefins are present, however, they compete for the Bronsted acid sites and form surface-bound alkoxide groups [53,54]. These alkoxy groups are relatively stable and reduce the coverage of the methoxy groups, resulting, consequently, in a lower DME consumption rate. The lower Brønsted acid strength of the iron with respect to aluminum zeolites is a key factor; lower acidity makes it more difficult for the alkoxides to form carbocation-like reaction intermediates needed for the MTH reaction. This competition for acid sites is a likely explanation for the inverse effect between isobutene addition and decreasing the DME consumption rate. An apparent activation energy was calculated for isobutene methylation using an Arrhenius plot (Supplemental Figure S5) and was determined to be 69.2 ± 6.7 kJ/mol. This is higher by at least 20 kJ/mol than values reported for apparent activation energies for methylation of both isobutene and n-butene over both aluminum ZSM-5 and about 10 kJ/mol higher than for the apparent activation energies reported for aluminum beta [32,55]. This higher activation energy is consistent with the lower acid strength of iron zeolites that would yield less stable (higher energy) transition states.

The 3.9% isobutene feed has the highest selectivity to C7 compounds, but the selectivity decreases as the amount of isobutene co-fed increases. This reduction in C7 selectivity could be

the C5 selectivity decreasing as the amount of isobutene co-fed decreases. In all cases isobutene methylation to a C5 olefin is still the main reaction and C5 maintains the highest selectivity but the subsequent methylations of the C5 olefins formed decreases as the amount of isobutene co-fed into the system increases.

To form pentenes, isobutene needs to be methylate one time; to form a C7 olefin, isobutene would undergo three methylations. An increase in C5s concentration would increase C5 surface alkoxides coverage competing with methoxy species and reducing the formation rate of C7 olefins. The increase in C8 selectivity as isobutene concentration increases, in contrast, could be due to an increase in dimerization rates that would increase at a rate order higher than 1 with respect to isobutene partial pressure.

The effect of temperature on the DME consumption rate during isobutene methylation is to increase DME consumption rate until a temperature of 340 °C is reached (Figure 6A). Above this temperature, however, there is rapid deactivation of the catalyst (Supplemental Figure S6), and consumption rate measurements are not reliable. This could be due to a change in the relative composition of the surface intermediates above this temperature: alkoxides can start to form carbocation-like intermediates, which can participate in hydride transfer reactions, and these can give rise to alkanes—the termination products in the olefin cycle—and to aromatic species that favor coke formation. At 360 °C and above, low aromatic concentrations (under 1%) of the observed carbon selectivity were detected. The carbon selectivity (Figure 6B) shows a marked increase in the methane concentration at higher temperatures from about 2% of the carbon selectivity at 340 °C and below to about 4% at 360 and increasing to about 18% at 400 °C. High methane selectivity has been reported in MTH chemistry once deactivation occurs from reactions of DME and methanol with formation of deposited carbonaceous products (coke) and from

decomposition reactions of methanol and DME being more favorable at higher temperatures [14,56].

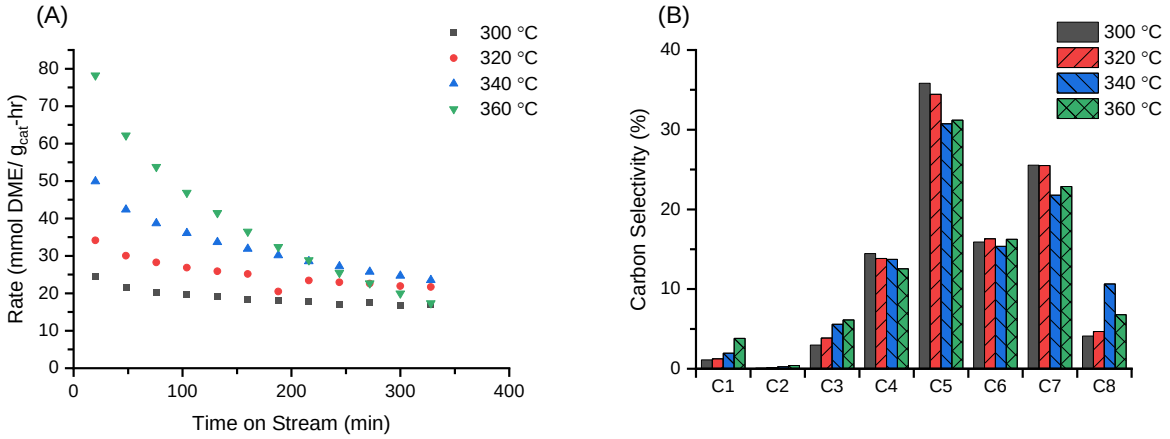

Figure 6 (A) DME consumption rate over H-[Fe]beta for the isobutene co-fed reaction with a 6.3% isobutene co-fed, 0.239 MPa, and WHSV 6.12 $g_{DME}g_{Catalyst}^{-1}hour^{-1}$ at different temperatures. (B) Carbon selectivity of isobutene co-fed over H-[Fe]beta at different temperatures at 216 minutes time on stream. Carbon balance at 216 minutes time on stream 300 °C 95%, 320 °C 95%, 340 °C 97%, and 360 °C 83%.

3.3 Olefin Cofeeding C5+ over H-[Fe]beta

C5 through C8 olefins (Figure 1) were co-fed with DME leading to a decrease in DME consumption rate as the size of the olefin increases (Figure 7A). These results support the previous observation that DME consumption rate decreased with increasing isobutene concentration due to the formation of surface alkoxides which compete with surface methoxy groups for surface sites. The C5-C8 olefins were most selective to C4 compounds (Figure 7B), particularly isobutene, consistent with the multiple methylations of the olefins until they cracked. The C8 olefins crack to form primarily C4 compounds, which is consistent with theoretical work by Plessow et al. [57] that showed, using theory, that for C8 olefins cracking rates have lower activation barriers than methylation, and thus crack faster than the rate at which they form. The selectivity of both the C7 and C8 olefins are very similar, that is the C7 olefin is methylated

rapidly to form a C8 olefin which then rapidly cracks to form smaller olefins. This is supported by the selectivity of the co-feeding a C7 olefin being 54% to C4 while having a selectivity of under 2% to C3. Note that no aromatics were detected under these reaction conditions. The selectivity of co-fed C5 and C6 olefins towards larger compounds compared to C2 and C3 formation rates suggest that methylation is faster than cracking for these compounds as well, as suggested by the report by Plessow et al. [57] where their theoretical work found that the barriers for cracking are significantly more than methylation for C5 and C6 olefins.

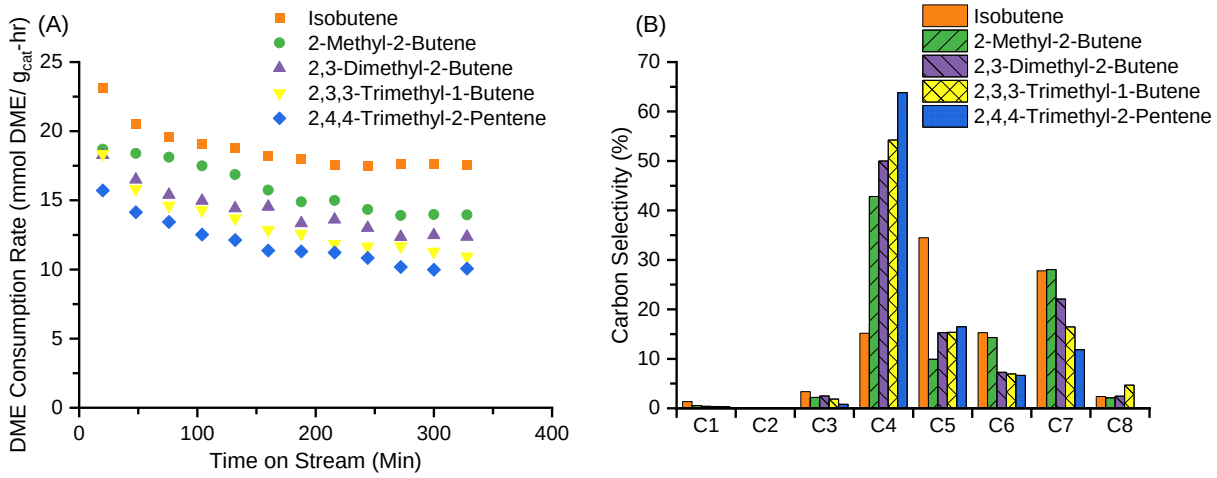

Figure 7 (A) DME consumption rate over H-[Fe]beta for different olefin co-feeds at 300 °C, 0.239 MPa, and WHSV 6.12 $g_{DME}g_{Catalyst}^{-1}hour^{-1}$ with olefin co-feeds of 3.9%. (B) Carbon selectivity of different olefin co-feeds over H-[Fe]beta with a 3.9% olefin co-fed after 216 minutes time on stream. Carbon selectivity does not include the co-fed olefin. Carbon balance after 216 minutes time on stream isobutene 100%, 2-methyl-2-butene 94%, 2,3-dimethyl-2-butene 94%, 2,3,3-trimethyl-1-butene 95%, and 2,4,4-trimethyl-2-pentene 93%.

3.4 Isobutene Methylation over Medium Pore H-[Fe]ZSM-5

As observed for Fe-beta, there is an increase in the DME consumption rate upon addition of isobutene to the feed stream over H-[Fe]ZSM-5 (Figure 8A). The carbon selectivity of MTH and isobutene co-fed with DME over H-[Fe]ZSM-5 (Figure8B) shifts away from ethylene and propylene and towards C5 to C8 olefins. In MTH chemistry, ethylene is often made through the

aromatic cycle but it can be made through the olefin cycle; propylene, in contrast, is a cracking product of the olefin cycle [28]. The change from cracking products towards larger olefins shows that methylation reaction rates are fast compared to cracking rates. The decrease in production rate of C2 and C3 olefins is also consistent with increased methylation rates as compared to MTH due to the formation of C5, C6, C7, C8 compounds that are generated continuously through the reactor. Hill et al. and Hill et al. [31,32] found that the apparent activation energy for methylation of ethylene and propylene is higher than for C4 and larger compounds.

The detection of aromatic compounds with an isobutene co-fed over Fe ZSM-5, as well as the presence of ethylene, shows that in this zeolite the aromatic cycle is not fully suppressed by the olefin co-fed. The carbon selectivity in Fe-ZSM-5 indicates that the olefin cycle TOF is faster than the aromatic TOF as larger olefins become the preferred products.

Fe-beta displays, on average, an increase in the DME consumption rate by a factor of ~2, when isobutene is co-fed, after 216 minutes time on stream for the remainder of the experiment. Whereas Fe-ZSM-5 shows an increase in the rate of only about 30% for the same TOS. On the other hand, H-[Fe]ZSM-5 has higher DME consumption rate with respect to H-[Fe]beta (Figure 8C) due to the higher heats of adsorption of DME and the olefins formed in the pores of ZSM-5 [54]. The difference in rates is probably not associated with particle size, Fe ZSM-5 had the larger particles but the faster rate as compared to Fe beta suggesting the difference in pore structure is more important than diffusion through the particles.

Fe-beta is selective to mostly C5 (36%) and C7 (25%); whereas Fe-ZSM-5 is selective to products in the C5-C8 (Figure 8D) range with selectivity of 19% for C5, 18% for C6, 15% for C7, and 12% for C8. The decrease in diffusion rates due to the smaller pore size in ZSM-5 is likely responsible for this difference. The olefin products spend more time in the zeolite pores

allowing for further methylation and cracking reactions as compared to more quickly diffusing out of the crystals of zeolite beta. This results in a more evenly distributed olefin pool by size (C5 to C8) accounting for 64% of the carbon selectivity in Fe-ZSM-5 as compared to a pool mostly of a C5 and C7 accounting for 61% of the carbon selectivity in Fe-beta. A broader olefin pool suggest that the methylation rates are not as dependent on what species are present and that faster interconversion via methylation reactions occurs. This is consistent with the results observed for different olefin co-feeds (see Supplemental Figure S7) over Fe-ZSM-5 giving a reaction rate not dependent on co-fed olefin size.

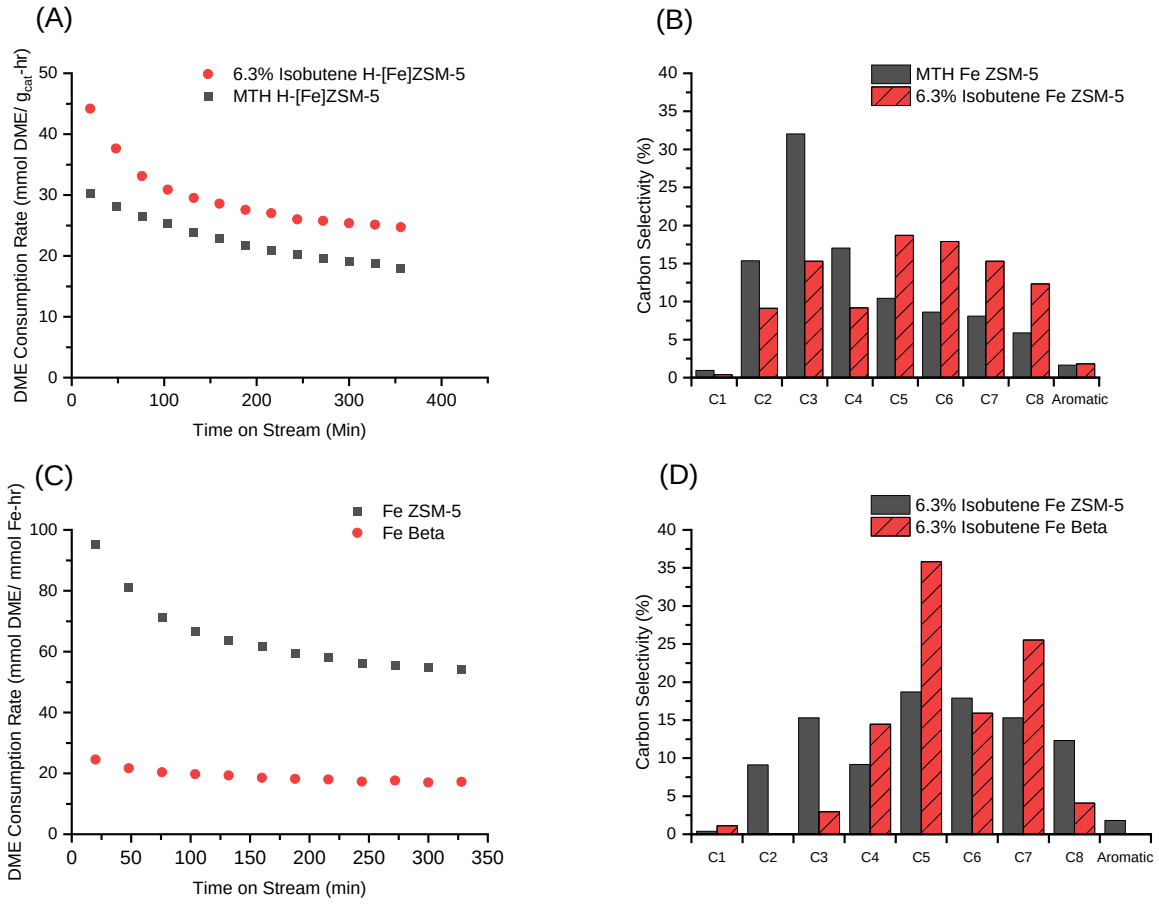

Figure 8 (A) DME consumption rate over H-[Fe]ZSM-5 for MTH and isobutene co-fed at 300 °C, 0.239 MPa, and WHSV 6.12 $g_{DME}g_{Catalyst}^{-1}hour^{-1}$, 6.3 % Isobutene co-fed. (B) Carbon selectivity for MTH and isobutene co-fed over H-[Fe]ZSM-5 after 216 minutes time on stream. (C) DME consumption rate over H-[Fe]ZSM-5 and H-[Fe]beta with an isobutene co-fed at 300

°C, 0.239 MPa, and WHSV 6.12 $g_{DME}g_{Catalyst}^{-1}hour^{-1}$, 6.3% isobutene co-fed. The reaction rate is normalized to mmol Fe to account for the different Si/Fe ratios for Fe ZSM-5 and Fe beta (D) Carbon selectivity for isobutene co-fed over H-[Fe]ZSM-5 and H-[Fe]beta after 216 minutes time on stream. Carbon selectivity does not include the co-fed olefin. Carbon balance after 216 minutes time on stream MTH Fe ZSM-5 92%, 6.3% isobutene co-fed Fe ZSM-5 94%, 6.3% isobutene co-fed Fe beta 95%.

3.5 Mechanistic Insights

The reaction analysis described above suggests that the reaction network leading to the formation of the main reaction products (Figure 9), is a subset of the reaction network proposed by Simonetti et al. [58] for the olefin cycle of MTH over aluminum beta. The key differences are an increase in the relative importance of isobutene dimerization and the effective absence of hydrogen transfer reactions which ultimately form alkanes and aromatics. One molecule of isobutene is fed into the system and then undergoes successive methylations by surface methoxy groups (CH_3*) until it is large enough to crack to form smaller olefins; most frequently two molecules of isobutene [59]. As the olefin intermediate size increases, methylation reactions are kinetically favored until C8 olefins are formed [57]. Once C8 is formed it preferentially cracks to form two molecules of isobutene [15].These isobutene molecules could then enter the methylation cycle again. Because for every molecule of isobutene two molecules of isobutene can be generated, this is stoichiometrically, a chain branching process. A run-away reaction does not occur because it is kinetically limited since the number of methylation sites is constant, and competition between surface methoxy groups and other alkoxides reduce overall methylation rates.

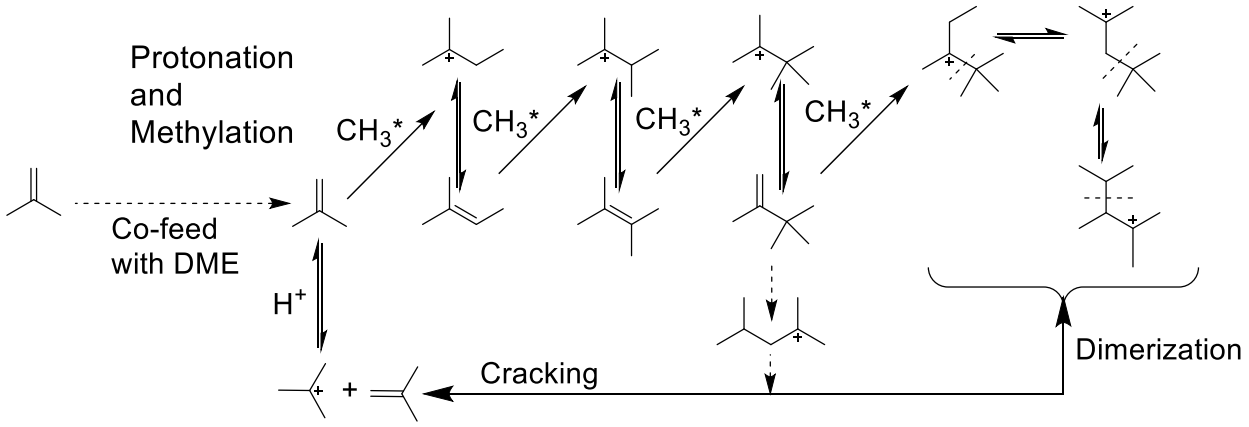

Figure 9 Proposed mechanism of olefin methylation reactions over H-[Fe]beta. CH_3* are surface methoxy groups.

4.0 Conclusion

Co-feeding isobutene with DME increased the rate of the MTH reaction over iron zeolites. Measured methylation rates were faster than dimerization or cracking rates in the 240-400°C range. However, this effect is concentration dependent and increasing the isobutene co-fed concentration above 6.3% reduced the reaction rate (that is, the rate order is negative after that point) probably due to competition for surface acid sites between olefins and surface methoxy groups that control methylation rate. The reaction rate decreased as the size of the co-fed olefin increased also due to surface coverage by the corresponding alkoxide species.

The effect of zeolite pore size is clearly observed on the selectivity of isobutene methylation, with the large pore Fe-beta being more selective to methylation product C5 and C7, whereas the medium pore Fe-ZSM-5 formed C5 to C8 olefins with similar selectivity but with decreasing selectivities from C5 through C8. The co-fed systems produced a mixture of C4 to C8 olefins with very small amounts of aromatics. Methylation beyond the olefins investigated herein (such as cyclic olefins) could be used to produce species not typically found in MTH processes. This would allow for the incorporation of methanol or other C1 compounds into a wider variety of hydrocarbons.

AUTHOR INFORMATION

Corresponding Author

*E-mail: lobo@udel.edu

ACKNOWLEDGMENT

This work was financially supported by the Catalysis Center for Energy Innovation, an Energy Frontier Research Center funded by the U.S. Department of Energy, Office of Science, Office of Basic Energy Sciences under Award Number DE-SC0001004.

References

[1] M. Stöcker, Microporous Mesoporous Mater. 29 (1999) 3–48.

[2] C.D. Chang, A.J. Silvestri, J. Catal. 47 (1977) 249–259.

[3] U. Olsbye, S. Svelle, M. Bjørgen, P. Beato, T.V.W. Janssens, F. Joensen, S. Bordiga, K.P. Lillerud, Angew. Chemie Int. Ed. 51 (2012) 5810–5831.

[4] M. Zhang, S. Xu, Y. Wei, J. Li, J. Chen, J. Wang, W. Zhang, S. Gao, X. Li, C. Wang, Z. Liu, RSC Adv. 6 (2016) 95855–95864.

[5] M.J. Chen, H.M. Feder, J.W. Rathke, J. Am. Chem. Soc. 104 (1982) 7346–7347.

[6] R.M. Dessau, R.B. LaPierre, J. Catal. 78 (1982) 136–141.

[7] I.M. Dahl, S. Kolboe, Catal. Letters 20 (1993) 329–336.

[8] I.M. Dahl, S. Kolboe, J. Catal. 149 (1994) 458–464.

[9] I.M. Dahl, S. Kolboe, J. Catal. 161 (1996) 304–309.

[10] W. Song, D.M. Marcus, H. Fu, J.O. Ehresmann, J.F. Haw, J. Am. Chem. Soc. 124 (2002) 3844–3845.

[11] J.F. Haw, W. Song, D.M. Marcus, J.B. Nicholas, Acc. Chem. Res. 36 (2003) 317–326.

[12] S. Ilias, A. Bhan, ACS Catal. 3 (2013) 18–31.

[13] H. Fu, W. Song, J.F. Haw, Catal. Letters 76 (2001) 89–94.

[14] H. Schulz, Catal. Today 154 (2010) 183–194.

[15] J.H. Ahn, B. Temel, E. Iglesia, Angew. Chemie - Int. Ed. 48 (2009) 3814–3816.

[16] J.H. Ahn, B. Temel, E. Iglesia, Process for Production of Triptane and Triptene, US7825287B2, 2009.

[17] N. Hazari, E. Iglesia, J.A. Labinger, D.A. Simonetti, Acc. Chem. Res. 45 (2012) 653–662.

[18] J.A. Schaidle, D.A. Ruddy, S.E. Habas, M. Pan, G. Zhang, J.T. Miller, J.E. Hensley, ACS Catal. 5 (2015) 1794–1803.

[19] C.T. Chu, C.D. Chang, J. Phys. Chem. 89 (1985) 1569–1571.

[20] D. Vitvarová, L. Kurfiřtová, M. Kubů, N. Žilková, Microporous Mesoporous Mater. 194 (2014) 174–182.

[21] M.A. Asensi, A. Corma, A. Martínez, M. Derewinski, J. Krysciak, S.S. Tamhankar, Appl. Catal. A Gen. 174 (1998) 163–175.

[22] M. Yabushita, H. Kobayashi, A. Neya, M. Nakaya, S. Maki, M. Matsubara, K. Kanie, A. Muramatsu, CrystEngComm 22 (2020) 7556–7564.

[23] A.J. Jones, R.T. Carr, S.I. Zones, E. Iglesia, J. Catal. 312 (2014) 58–68.

[24] T. Inui, H. Matsuda, O. Yamase, H. Nagata, K. Fukuda, T. Ukawa, A. Miyamoto, J. Catal. 98 (1986) 491–501.

[25] Y. Jin, S. Asaoka, S. Zhang, P. Li, S. Zhao, Fuel Process. Technol. 115 (2013) 34–41.

[26] K.Y. Lee, S.W. Lee, S.K. Ihm, Ind. Eng. Chem. Res. 53 (2014) 10072–10079.

[27] S. Svelle, O.P. Rønning, S. Kolboe, J. Catal. 224 (2004) 115–123.

[28] S. Svelle, F. Joensen, J. Nerlov, U. Olsbye, K.P. Lillerud, S. Kolboe, M. Bjørgen, J. Am. Chem. Soc. 128 (2006) 14770–14771.

[29] D.A. Simonetti, J.H. Ahn, E. Iglesia, ChemCatChem 3 (2011) 704–718.

[30] I. Hill, A. Malek, A. Bhan, ACS Catal. 3 (2013) 1992–2001.

[31] I.M. Hill, S. Al Hashimi, A. Bhan, J. Catal. 285 (2012) 115–123.

[32] I.M. Hill, Y.S. Ng, A. Bhan, ACS Catal. 2 (2012) 1742–1748.

[33] S. Ilias, A. Bhan, J. Catal. 290 (2012) 186–192.

[34] Y. Xue, J. Li, S. Wang, X. Cui, M. Dong, G. Wang, Z. Qin, J. Wang, W. Fan, J. Catal. 367 (2018) 315–325.

[35] X. Sun, S. Mueller, Y. Liu, H. Shi, G.L. Haller, M. Sanchez-Sanchez, A.C. Van Veen, J.A. Lercher, J. Catal. 317 (2014) 185–197.

[36] X. Sun, S. Mueller, H. Shi, G.L. Haller, M. Sanchez-Sanchez, A.C. Van Veen, J.A. Lercher, J. Catal. 314 (2014) 21–31.

[37] W. Wu, W. Guo, W. Xiao, M. Luo, Chem. Eng. Sci. 66 (2011) 4722–4732.

[38] X. Huang, D. Aihemaitijiang, W. De Xiao, Chem. Eng. J. 286 (2016) 150–164.

[39] M. Westgård Erichsen, K. De Wispelaere, K. Hemelsoet, S.L.C. Moors, T. Deconinck, M.

Waroquier, S. Svelle, V. Van Speybroeck, U. Olsbye, J. Catal. 328 (2015) 186–196.

[40] G.A.V. Martins, G. Berlier, S. Coluccia, H.O. Pastore, G.B. Superti, G. Gatti, L. Marchese, J. Phys. Chem. C 111 (2007) 330–339.

[41] N. Katada, K. Nouno, J.K. Lee, J. Shin, S.B. Hong, M. Niwa, J. Phys. Chem. C 115 (2011) 22505–22513.

[42] A. Raj, S. Sivasanker, K. Lázár, J. Catal. 147 (1994) 207–213.

[43] J.H. Yun, R.F. Lobo, J. Catal. 312 (2014) 263–270.

[44] M.M.J. Treacy, J.B. Higgins, in: M.M.J. Treacy, J.B.B.T.-C. of S.X.R.D.P.P. for Z. (Fifth E. Higgins (Eds.), Collect. Simulated XRD Powder Patterns Zeolites, Fifth, Elsevier Science B.V., Amsterdam, 2007, pp. 278–279.

[45] M. Thommes, K. Kaneko, A. V. Neimark, J.P. Olivier, F. Rodriguez-Reinoso, J. Rouquerol, K.S.W. Sing, Pure Appl. Chem. 87 (2015) 1051–1069.

[46] M.A. Camblor, A. Corma, S. Valencia, J. Mater. Chem. 8 (1998) 2137–2145.

[47] D. Goidfaib, M. Bernardo, K.G. Strohmaier, D.E.W. Vaughan, H. Thomann, J. Am. Chem. Soc. 116 (1994) 6344–6353.

[48] D.H. Lin, G. Coudurier, J.C. Vedrine, Stud. Surf. Sci. Catal. 49 (1989) 1431–1148.

[49] J. Patarin, Tuilier, J. Durr, H. Kessler, Zeolites 12 (1992) 70–75.

[50] S. Bordiga, R. Buzzoni, F. Geobaldo, C. Lamberti, E. Giamello, A. Zecchina, G. Leofanti, G. Petrini, G. Tozzola, G. Vlaic, J. Catal. 158 (1996) 486–501.

[51] J.W. Yoon, J.S. Chang, H. Du Lee, T.J. Kim, S.H. Jhung, J. Catal. 245 (2007) 253–256.

[52] K. Hauge, E. Bergene, D. Chen, G.R. Fredriksen, A. Holmen, Catal. Today 100 (2005) 463–466.

[53] M. Boronat, P.M. Viruela, A. Corma, J. Am. Chem. Soc. 126 (2004) 3300–3309.

[54] R. Gounder, E. Iglesia, Chem. Commun. 49 (2013) 3491–3509.

[55] S. Svelle, P. Ola, U. Olsbye, S. Kolboe, J. Catal. 234 (2006) 385–400.

[56] W. Zhao, B. Zhang, G. Wang, H. Guo, J. Energy Chem. 23 (2014) 201–206.

[57] P.N. Plessow, F. Studt, Catal. Sci. Technol. 8 (2018) 4420–4429.

[58] D.A. Simonetti, J.H. Ahn, E. Iglesia, J. Catal. 277 (2011) 173–195.

[59] J.H. Ahn, B. Temel, E. Iglesia, Angew. Chem. Int. Ed. 48 (2009) 3814–3816.